

Precipitation of Submicrometer-Sized Poly(methyl methacrylate) Particles with a Compressed Fluid Antisolvent

I-Hsiang Lin, Pei-Fang Liang, Chung-Sung Tan

Department of Chemical Engineering, National Tsing Hua University, Hsinchu, Taiwan 30013, Republic of China

Received 5 August 2009; accepted 8 December 2009

DOI 10.1002/app.31975

Published online 26 March 2010 in Wiley InterScience (www.interscience.wiley.com).

ABSTRACT: Submicrometer-sized poly(methyl methacrylate) (PMMA) particles were generated by precipitation with a compressed fluid antisolvent technique. The precipitation was carried out as follows. A solution containing PMMA was sprayed through a nozzle into a precipitator. The antisolvent CO₂ was continuously passed through the precipitator during the operation at a flow rate of 2000 mL/min. When toluene was used as the solvent, scanning electron microscopy images showed that solid, spherical PMMA particles with less coalescence could be generated only when both vapor and liquid CO₂ was present and the liquid CO₂ level in the precipitator was one-eighth. The morphology and size of the precipitated PMMA were found to be dependent on the solvents. Toluene, which had the lowest solubility parameter,

was the most appropriate solvent in comparison with tetrahydrofuran, acetone, and nitromethane. More uniform submicrometer-sized PMMA particles were obtained at PMMA concentrations equal to or less than 1.0 wt % in the toluene solution. A narrower particle size distribution was observed for precipitating PMMA with a molecular weight of 85,000 versus PMMA with a molecular weight of 36,000. To generate PMMA particles with less coalescence, liquid CO₂ instead of supercritical CO₂ was suggested for use in drying immediately after the spraying of the PMMA solution. © 2010 Wiley Periodicals, Inc. *J Appl Polym Sci* 117: 1197–1207, 2010

Key words: morphology; particle size distribution; separation techniques; thermoplastics; yielding

INTRODUCTION

Techniques using a supercritical or compressed fluid to generate ultrafine particles have received widespread attention in recent years.^{1–4} Generally, they can be classified into two categories: rapid expansion of a supercritical solution^{5–9} and precipitation with a compressed fluid antisolvent (PCA).^{10–17} The commonly used gas antisolvent and supercritical antisolvent (SAS) techniques are included in the latter category. The application of rapid expansion of a supercritical solution is generally limited by the low solubility of the polymer in the supercritical fluid and the need for a high operating pressure. In antisolvent operations, an antisolvent should be chosen such that it can be dissolved into a solvent but cannot solubilize the solute, which will be precipitated to a large extent. The dissolution of an antisolvent in a liquid organic solvent expands the solvent and therefore weakens the interaction between the sol-

vent and solute. As a result, precipitation of the solute from the solvent occurs. This operation, especially when compressed CO₂ is used as an antisolvent, generally takes place at temperatures not far from room temperature. As a result, it is more suitable for the treatment of heat-sensitive materials than the conventional evaporation method. In addition, compressed CO₂ is released from the precipitated materials after the reduction of the pressure to the atmospheric level, and this leads subsequently to easy separation.

Reverchon et al.¹⁸ used SAS to generate poly(methyl methacrylate) (PMMA) particles through a nozzle with a diameter ranging from 60 to 200 μm. For operations in the pressure range of 7.2–8.5 MPa, the temperature range of 308–320 K, and the PMMA concentration range of 0.68–1.27 wt %, micrometer-sized, hollow-core-structure PMMA particles (called expanded microparticles by the authors) could be generated with solvents such as acetone, tetrahydrofuran (THF), methyl methacrylate, and chloroform. The authors proposed that the mechanism for the formation of the expanded microparticles was as follows: PMMA preferentially precipitated at the droplet surface at which the highest expansion existed after the dissolution of CO₂ into the liquid droplet. Obviously, the temperature and pressure, which affected the degree of expansion, the droplet size,

Correspondence to: C.-S. Tan (cstan@mx.nthu.edu.tw).

Contract grant sponsor: National Science Council of Republic of China; contract grant number: NSC98-ET-1-007-008-ET.

and the PMMA concentration were the determining variables. Vega et al.,¹⁹ however, obtained fibrous PMMA instead of particles by spraying 1.0 wt % PMMA in a dichloromethane solution into a supercritical CO₂ environment through a swirl nozzle with a diameter of 100 μm at 313 K and 11 MPa. With ultrasound, Zhang et al.²⁰ produced PMMA capsules rather than particles from a cyclohexane solution with a high PMMA concentration in a batch operation with CO₂ as the antisolvent at 301 K and 6.20 MPa.

To avoid flocculation of the generated PMMA microparticles, Mawson et al.²¹ added a copolymer stabilizer to liquid CO₂ at 296 K and 12.41 MPa or a polymer solution before they sprayed the polymer solution and CO₂ through a coaxial nozzle. PMMA particles of 0.1–0.5 μm were generated when the stabilizer was present in liquid CO₂, and larger PMMA particles ranging from 0.5 to 2 μm were generated when the stabilizer was present in the polymer solution. Young et al.²² obtained biodegradable polymer microspheres encapsulated with lysozyme from a dichloromethane solution in a continuous PCA process. In the process, both vapor and liquid CO₂ coexisted in the precipitator. They observed that precipitated polymer particles with less agglomeration were generated at lower temperatures. Fan and Tan²³ generated a solid cyclo-olefin copolymer (COC) from a toluene solution with compressed CO₂ as the antisolvent in a continuous PCA operation. They found that COC microspheres could be generated only in an operation in which both vapor and liquid CO₂ coexisted. This was also the case for the precipitation of polystyrene with 1,1,1,2-tetrafluoroethane (HFC-134a) as the antisolvent.²⁴

Because of the good biocompatibility and transparency of PMMA, nonaggregated PMMA particles have been used extensively for biomedical²⁵ and optical materials.²⁶ The previous description makes it obvious that a different phase of an antisolvent will lead to a different morphology of precipitated PMMA in a PCA process. Besides, PMMA particles without coalescence cannot be easily obtained in a PCA process because of the severe plasticization of PMMA in the presence of compressed CO₂.²² The objective of this study was, therefore, to determine if solid, spherical, submicrometer-sized PMMA particles without coalescence in the absence of a stabilizer could be generated in a continuous PCA operation in which both liquid and vapor phases of the antisolvent CO₂ existed. The effects of operation variables, including the temperature, pressure, liquid CO₂ level in the precipitator, PMMA molecular weight (MW), PMMA concentration, and drying conditions, on the morphology and size of the precipitated PMMA were examined. It is known that the solvating power of a solvent for a polymer depends on its solubility parameter (δ). A small dif-

ference in δ between a polymer and a solvent is generally favorable for the dissolution of the polymer in the solvent.^{27–29} The addition of compressed CO₂ to a polymer solution would increase the difference in δ between the solvent and polymer. As a result, precipitation of the polymer from the solution would occur. The other objective of this study was, therefore, to examine the effects of solvents with different δ values on the morphology and particle size distribution (PSD) of precipitated PMMA.

EXPERIMENTAL

Materials

PMMA with MWs of 85,000 and 36,000 were purchased from Aldrich (Milwaukee, WI) and Acros Organics (Morris Plains, NJ), respectively. Toluene with a purity of 99.97% and acetone with a purity of 99.9% were purchased from Echo Chemical (Miaoli, Taiwan). THF with a purity of 99.8% was purchased from Tedia Co. (Fairfield, OH). Nitromethane with a purity of 99% was purchased from Acros Organics, and CO₂ with a purity of 99.5% was purchased from Boclh Industrial Gases (Taipei, Taiwan). All chemicals were used as received.

Apparatus and operation

The experimental apparatus used to generate submicrometer-sized PMMA particles from a sprayed solution with CO₂ as the antisolvent is shown in Figure 1. The precipitator, made of 316 stainless steel, had an inside diameter of 0.05 m and a total volume of 600 mL, and it was equipped with visual windows. To collect the precipitated particles, a filter film with a pore size of 0.45 μm (HVHP4700, Millipore, Billerica, MA) was placed onto a 100-mesh stainless steel sieve located at the bottom of the precipitator. The

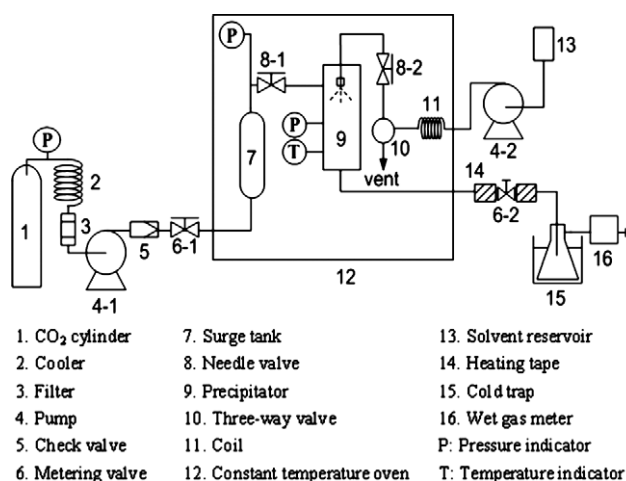


Figure 1 Experimental apparatus for the precipitation of the PMMA particles.

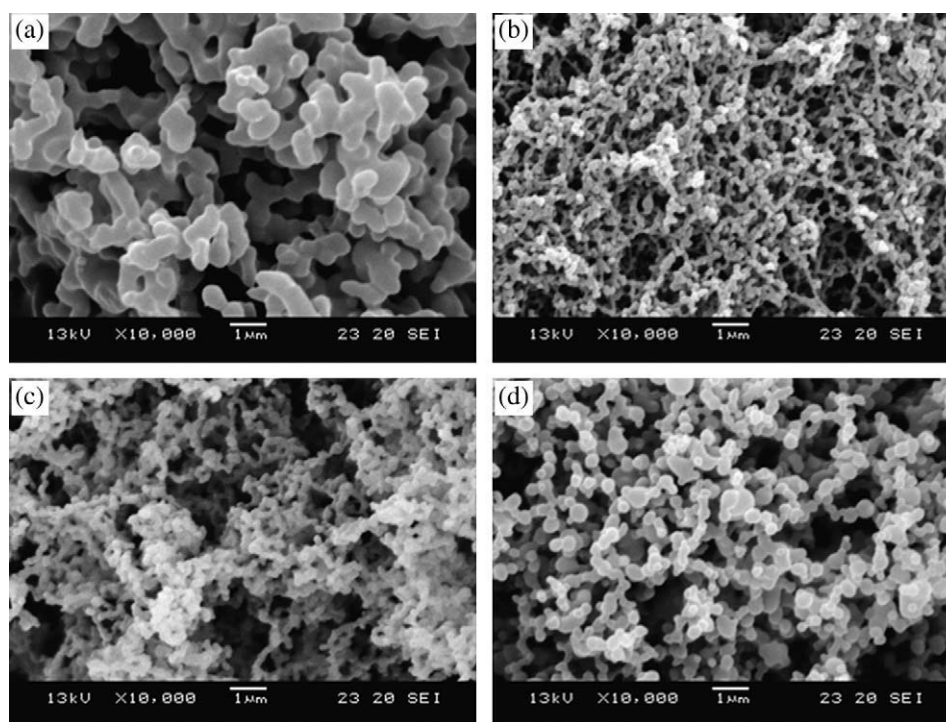


Figure 2 SEM images of the precipitated PMMA particles for a PMMA concentration of 1 wt % and a PMMA MW of 85,000 at temperatures and pressures of (a) 298 K and 6.21 MPa, (b) 298 K and 8.28 MPa, (c) 308 K and 8.97 MPa, and (d) 298 K and 6.41 MPa.

precipitator was kept in a constant-temperature oven whose temperature could be controlled within ± 0.2 K.

In the operation, a high-pressure pump (MD46, Milton Roy, Pont-Saint-Pierre, France) was used to deliver the compressed CO_2 . The volumetric flow rate of the compressed CO_2 was controlled with a needle valve and a metering valve located at the entrance and exit of the precipitator, respectively, as shown in Figure 1. The flow rate of CO_2 , maintained at 2000 mL/min, was monitored with a wet gas meter (W-NK-1, Shinagawa, Tokyo, Japan) located downstream of the precipitator. When liquid and vapor CO_2 coexisted in the precipitator, the liquid CO_2 level could be observed visually and controlled to a desired level by the simultaneous adjustment of the needle valve and the metering valve. A predetermined PMMA concentration in solution was prepared first, and then the solution was introduced into the precipitator through a nozzle with an inner diameter of 0.25 mm by a high-performance liquid chromatography pump (3200, Consta Metric, Riviera Beach, FL). The feed rate of the solution to the precipitator was maintained at 5 mL/min in all the runs. The pressure drop across the nozzle was observed to be about 0.7 MPa. The solution, drained from the bottom of the precipitator, was collected with a cold trap in which the temperature was maintained at 263 K. After the spraying of the solution was finished, the compressed CO_2 continuously

flowed through the precipitator for 2 h to remove the solvent retained on the precipitated materials. After this drying operation, the pressure in the precipitator was gradually reduced to the atmospheric level, and the materials that precipitated onto the filter and the wall of the precipitator were collected. The collected PMMA particles were subsequently heated in a vacuum oven at 313 K overnight to remove possible residual solvent within the particles before analysis. The size and morphology of the collected PMMA particles did not vary after the low-temperature treatment in the vacuum oven, and no difference in the glass-transition temperature was observed for the PMMA particles before and after the PCA process. The PMMA particles, after heating, were also weighed to calculate the yield in each operation. The yield was defined as the amount of PMMA collected on the filter paper and from the wall of the precipitator divided by the injected mass of PMMA.

Characterization

The morphology of the precipitated PMMA was characterized with a JSM-5600 scanning electron microscope (JEOL, Tokyo, Japan), and the PSD of the collected PMMA was determined with built-in size analysis software in the scanning electron microscope. About 200 particles were used in the determination of the PSD. For the scanning electron microscopy (SEM) measurements, the samples were spread onto

carbon tape and coated with a thin layer of gold. The MW of the precipitated PMMA was determined with a gel permeation chromatograph equipped with a Waters (Milford, MA) 510 pump, a Waters 410 differential refractometer, and a series of 50-, 10³-, and 10⁴-Å Phenogel columns (Phenomenex, Torrance, CA).

RESULTS AND DISCUSSION

Effects of the temperature and pressure

The reproducibility tests were performed at various temperatures and pressures. Almost the same morphology and size for the collected PMMA (determined from SEM images) and nearly the same yield were observed, and this indicated the reliability of the operation. After extensive study in different temperature and pressure ranges with toluene as the solvent, solid, submicrometer-sized PMMA particles without coalescence could be generated only in the operations in which both vapor and liquid CO₂ coexisted in the precipitator and the liquid level was maintained at a certain level in the precipitator, as shown in Figure 2(d). For the operation in which only vapor CO₂ existed in the precipitator at 298 K [Fig. 2(a)], the solution was atomized to fine droplets after being sprayed into the precipitator via a nozzle. During the path of the fine droplets in the vapor CO₂, mutual diffusion occurred simultaneously.²² CO₂ diffused into droplets and swelled the solution; at the same time, the solvent also diffused out of the droplets and into the CO₂ stream. Therefore, the nucleation of the polymer-rich phase within the fine droplets began to occur. Because the removal rate of the solvent within the droplets was not high enough on account of the lower extraction rate of the solvent with vapor CO₂, the fine droplets that formed adhered together, and agglomerates of PMMA were thus formed.

When the pressure was increased from 6.21 to 8.28 MPa, at which only liquid CO₂ was present in the precipitator, the observed interconnected network structure [Fig. 2(b)] was believed to result from the relatively poor formation of fine droplets after the solution left the nozzle due to the higher density of liquid CO₂. This explanation might apply to the SAS operation as well because precipitated PMMA of a similar structure was formed [Fig. 2(c)]. Solid, submicrometer-sized PMMA particles, instead of expanded PMMA microparticles, were generated, and this indicated the smaller droplet sizes in this SAS operation. For the operation in which both vapor and liquid CO₂ existed in the precipitator and the liquid CO₂ level in the precipitator was one-quarter, precipitation was not observed visually in the vapor CO₂ phase; however, temporary turbidity caused by the precipitated PMMA was observed when the solution fell into the liquid CO₂. From this observation and the generation of more individual submicrometer-

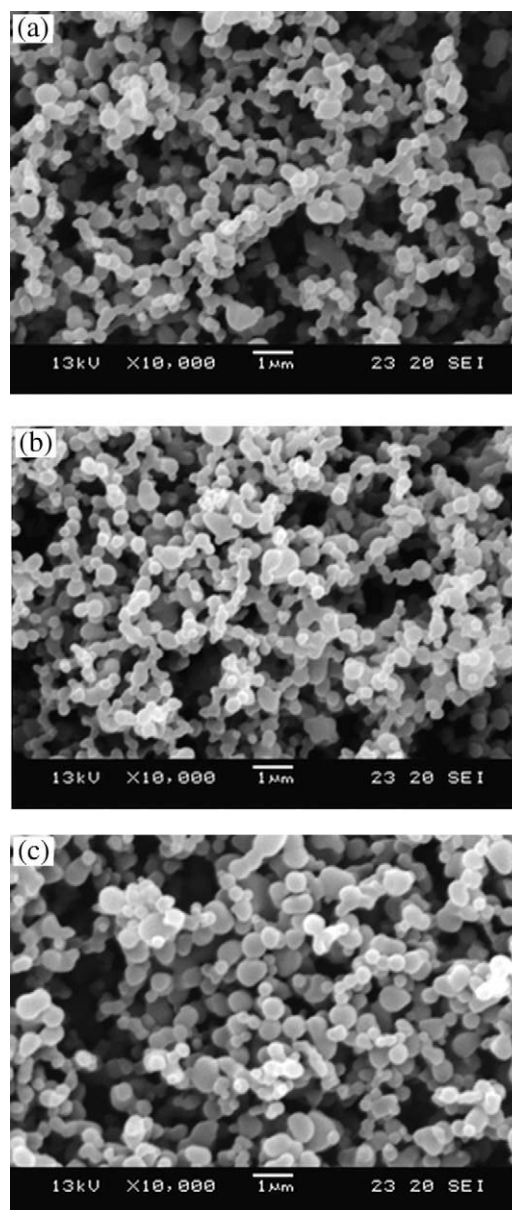


Figure 3 SEM images of the precipitated PMMA particles for a PMMA concentration of 1 wt %, a PMMA MW of 85,000, a pressure of 6.41 MPa, a temperature of 298 K, and a liquid CO₂ level in the precipitator of (a) one-half, (b) one-fourth, and (c) one-eighth.

sized PMMA particles with less coalescence [Fig. 2(d)], the nucleation and growth mechanism in which nucleation mainly occurs in the vapor phase and growth occurs in the liquid phase^{23,24} seems to apply to this operation. Because solid, spherical, submicrometer-sized PMMA particles were the desired morphology, the operation in which the vapor and liquid coexisted was chosen for further study.

Effect of the liquid CO₂ level

With a PMMA MW of 85,000, a PMMA concentration in toluene of 1.0 wt %, a temperature of 298 K, and a

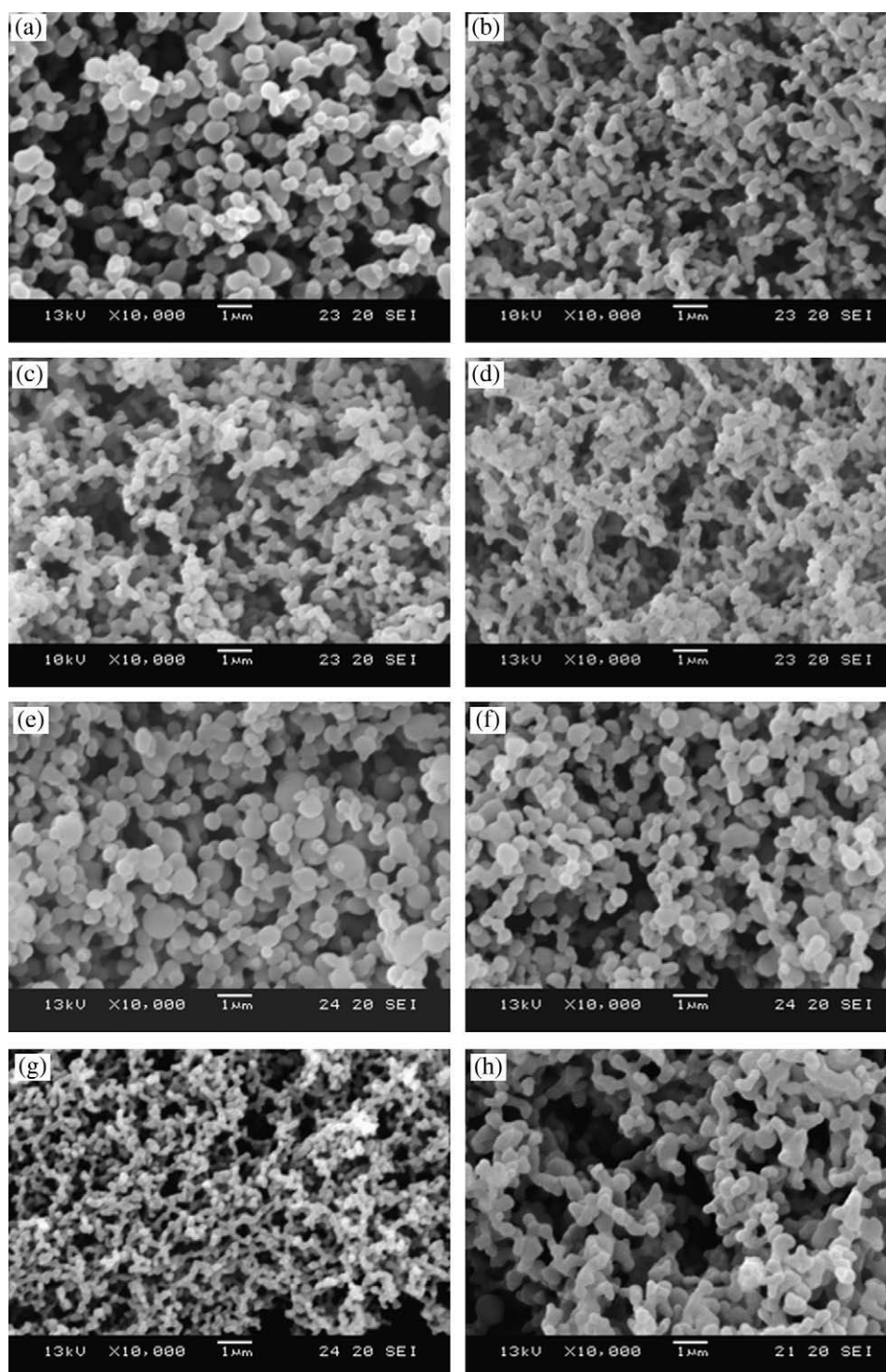


Figure 4 SEM images of the precipitated PMMA particles for a PMMA concentration of 1 wt %, a temperature of 298 K, a pressure of 6.41 MPa, and a liquid CO₂ level in the precipitator of one-eighth for solvents and PMMA MWs of (a) toluene and 85,000, (b) THF and 85,000, (c) acetone and 85,000, (d) nitromethane and 85,000, (e) toluene and 36,000, (f) THF and 36,000, (g) acetone and 36,000, and (h) nitromethane and 36,000.

pressure of 6.41 MPa, Figure 3 shows that submicrometer-sized and nearly spherical particles without coalescence could be generated at a liquid CO₂ level of one-eighth in the precipitator, and severe coalescence of the precipitated particles was found to occur at a

liquid CO₂ level of one-half. A possible reason for the requirement of a longer vapor space to form particles with less coalescence is that nucleation occurred in the vapor space, and growth occurred in liquid CO₂. Longer travel of the sprayed droplets of the PMMA

TABLE I
Effects of the Solvent and PMMA MW on the Yield and Morphology at 298 K and 6.41 MPa with a PMMA Concentration of 1 wt % and a Liquid CO₂ Level in the Precipitator of One-Eighth

Solvent	PMMA MW	Yield (wt %)	Morphology
Toluene	85,000	93.2	Submicrometer spheres
THF	85,000	90.1	Coalescence
Acetone	85,000	88.3	Coalescence
Nitromethane	85,000	91.8	Agglomeration
Toluene	36,000	93.6	Submicrometer spheres
THF	36,000	89.5	Submicrometer spheres with slight coalescence
Acetone	36,000	86.4	Coalescence
Nitromethane	36,000	91.1	Coalescence

solution in the vapor CO₂ phase depleted more PMMA for nucleation. As a result, less growth occurred when the droplets fell into the liquid CO₂ phase, and this yielded less coalescence.

Effects of the solvent and PMMA MW

The SEM images in Figure 4 and Table I illustrate the effects of the solvent and MW on the morphology of the collected PMMA particles. Spherical, submicrometer-sized PMMA particles without coalescence could be generated only from the toluene solution with PMMA MWs of 85,000 and 36,000 in

TABLE II
 δ Values of the PMMA and Solvents^{27,28}

Solvent and solute	δ (MPa ^{0.5})
Toluene	18.2
THF	19.4
Acetone	20.1
Nitromethane	25.1
PMMA	22.7

the operation with a CO₂ level of one-eighth, as shown in Figure 4 and Table I. When THF, acetone, and nitromethane were used as the solvents, PMMA particles with coalescence and even agglomeration were observed in the operation with both PMMA MWs, as shown in Figure 4. The reason for the superiority of toluene to other solvents may be its δ value, which is the lowest. Table II lists the δ values for all the solvents used and PMMA. In general, a large affinity between a solute and a solvent exists when their δ values are sufficiently close. Phase separation will occur facily as the difference in δ increases. The δ values of liquid and vapor CO₂ are 12.4 and 4.2 MPa^{0.5}, respectively, at 298 K and 6.41 MPa (as calculated with an equation in the literature).²⁹ The dissolution of CO₂ into a solvent will form a CO₂-expanded solvent.³⁰ The δ of this CO₂-expanded solvent should be smaller than that of the solvent if the δ value of CO₂ is smaller than that of the solvent, and it should become smaller when

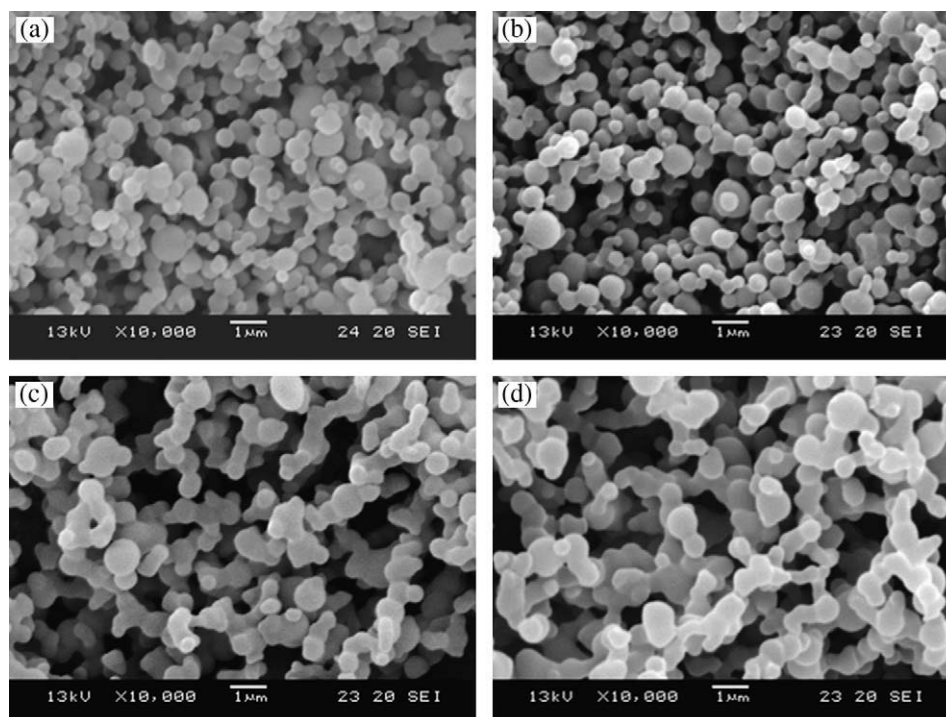


Figure 5 SEM images of the precipitated PMMA particles for a PMMA concentration of 1 wt %, a temperature of 298 K, a pressure of 6.41 MPa, and a liquid CO₂ level in the precipitator of one-eighth for CO₂ drying at temperatures and pressures of (a) 298 K and 6.41 MPa, (b) 298 K and 8.97 MPa, (c) 308 K and 8.97 MPa, and (d) 308 K and 10.3 MPa.

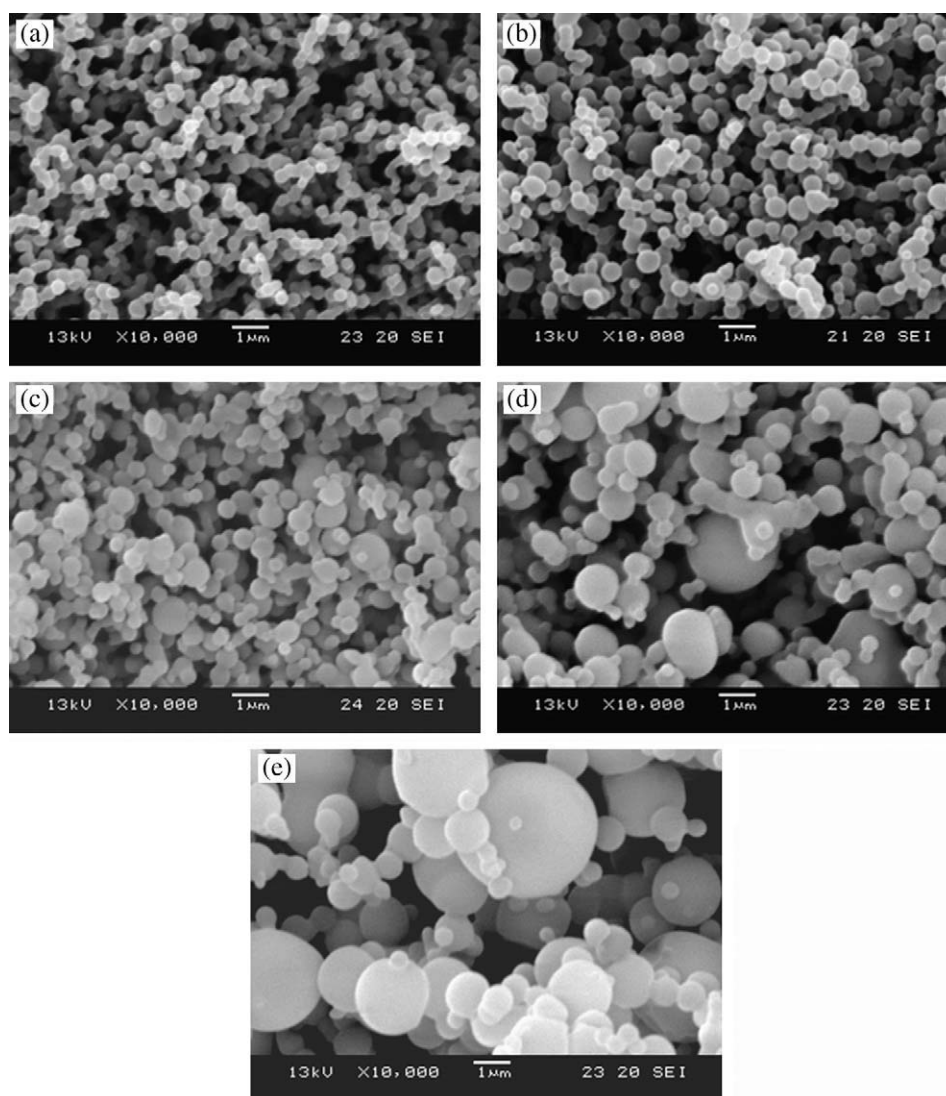


Figure 6 SEM images of the precipitated PMMA particles for a PMMA MW of 36,000, a temperature of 298 K, a pressure of 6.41 MPa, a liquid CO₂ level in the precipitator of one-eighth, and PMMA concentrations of (a) 0.4, (b) 0.72, (c) 1, (d) 2, and (e) 4 wt %.

more CO₂ is dissolved into the solvent.²⁹ As a result, the dissolved solute will be precipitated. Because toluene possesses the lowest δ values among the solvents used, nucleation more easily occurred in the vapor CO₂ space in comparison with the other solvents because of the largest difference in δ between the PMMA and solvent after the dissolution of CO₂ into the solvent. The faster nucleation consequently led to less growth of the PMMA particles when they hit the liquid CO₂ in the precipitator. In this situation, particles with less coalescence were generated. Acetone is a very good solvent for PMMA³¹ because its δ value is sufficiently close to that of PMMA. Although the dissolution of CO₂ into acetone also resulted in a larger difference in δ , the difference was not as large as that with toluene as the solvent. In this situation, the precipitated particles exhibited a smaller size and severe coalescence.

Small PMMA particle sizes and large coalescence were found to occur with a PMMA MW of 36,000, as shown in Figure 4. This was because the affinity between acetone and PMMA with an MW of 36,000 was higher than that between acetone and PMMA with an MW of 85,000. As a result, the nucleation with the MW of 36,000 occurred later in comparison with that with the MW of 85,000. When THF with a δ value lying between those of toluene and acetone was used for precipitating PMMA with an MW of 36,000, the average size of the collected PMMA particles was shown to be slightly smaller than that of the particles in the PMMA/toluene system but larger than that of those in the PMMA/acetone system. Besides, the morphology of the collected PMMA particles from THF was observed to lie between those of the particles from toluene and acetone. The differences in the size and morphology mainly resulted from the

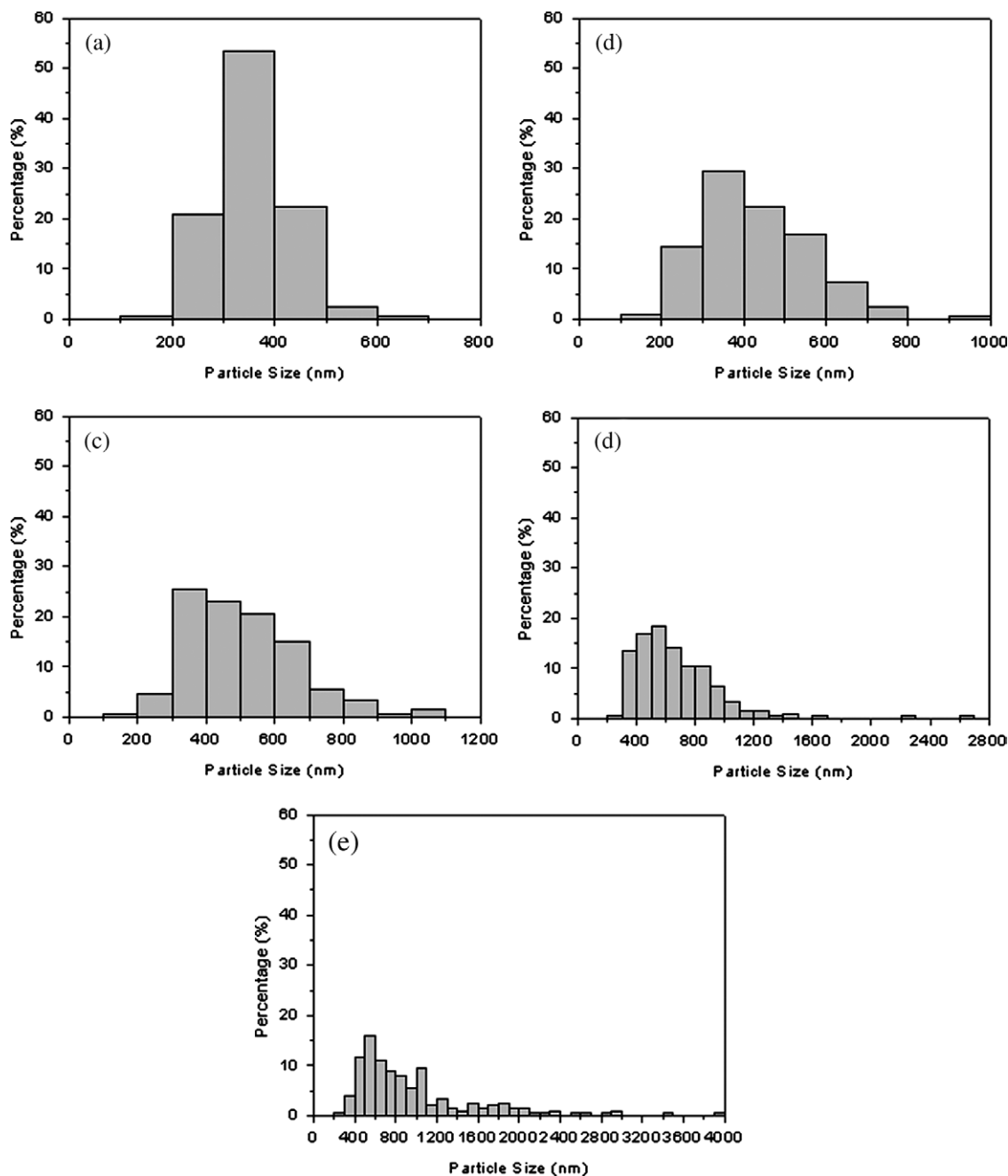


Figure 7 PSD of the precipitated PMMA particles for a PMMA MW of 36,000, a temperature of 298 K, a pressure of 6.41 MPa, a liquid CO₂ level of one-eighth of the precipitator, and PMMA concentrations of (a) 0.4, (b) 0.72, (c) 1, (d) 2, and (e) 4 wt %.

differences in the affinity between PMMA and solvents. However, for the PMMA with an MW of 85,000, the morphologies of the collected PMMA particles from THF and acetone were found not to be very different, as shown in Figure 4. This was probably because the precipitation rates of PMMA from these two solvents were nearly the same because phase separation more easily occurs for a polymer with a higher MW after the dissolution of CO₂ into solution. When nitromethane was used as the solvent, more agglomeration of the collected PMMA was

observed. This was because nitromethane possesses a δ value higher than that of PMMA. In this situation, the difference in δ between nitromethane and PMMA after the introduction of CO₂ was smaller than that with other solvents. As a result, growth instead of nucleation became dominant in the precipitation. We therefore conclude that a solvent possessing a δ value higher than that of PMMA is not a suitable solvent in PCA with CO₂ as the antisolvent.

In addition to the particle size and morphology, the yield was also found to be dependent on the

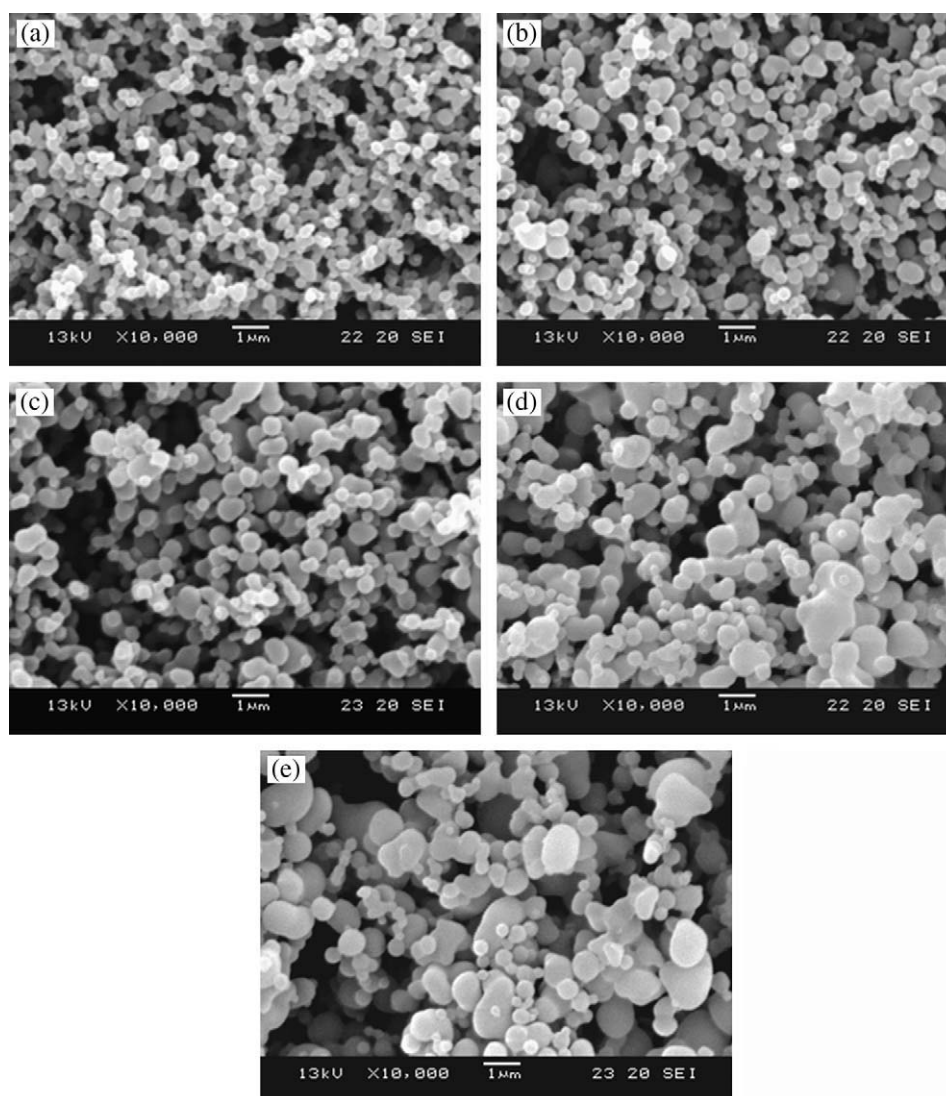


Figure 8 SEM images of the precipitated PMMA particles for a PMMA MW of 85,000, a temperature of 298 K, a pressure of 6.41 MPa, a liquid CO₂ level in the precipitator of one-eighth, and PMMA concentrations of (a) 0.4, (b) 0.72, (c) 1, (d) 2, and (e) 4 wt %.

solvent in this operation. Table I shows that 100% of the collection of the precipitated PMMA was not achieved because some PMMA was drained from the precipitator with the solvent. This portion of PMMA, however, could be collected in the cold trap located downstream of the precipitator. The total amounts of the PMMA collected in the precipitator and in the cold trap were found to be sufficiently close to the injected amount of PMMA. Besides, the standard deviations of the PMMA yields under various operation conditions were observed to be less than 3 wt %, and this indicated the reliability of this operation. It can also be seen from Table I that the highest yield happened in the operation with toluene as the solvent. This is because toluene has the smallest δ value, which leads to higher supersaturation after the dissolution of CO₂. On the basis of the obtained morphology, size, and yield of the precipi-

tated PMMA, the use of δ for the selection of the solvent in the antisolvent operation is suggested.

Effect of the drying conditions

The effect of the drying conditions on the morphology and size of the collected PMMA was also examined in this study. Although CO₂ was absorbed by PMMA during the drying with compressed CO₂, PMMA foams were not observed with slow expansion of the pressurized CO₂ after the drying. For the precipitation of PMMA with an MW of 36,000 from a toluene solution with 1.0 wt % PMMA in a precipitator with a liquid CO₂ level of one-eighth, Figure 5 shows SEM images of the collected PMMA particles dried with different phases of CO₂ after spraying, including liquid CO₂ with a density of 0.71 g/cm³ at the same temperature and pressure used in the

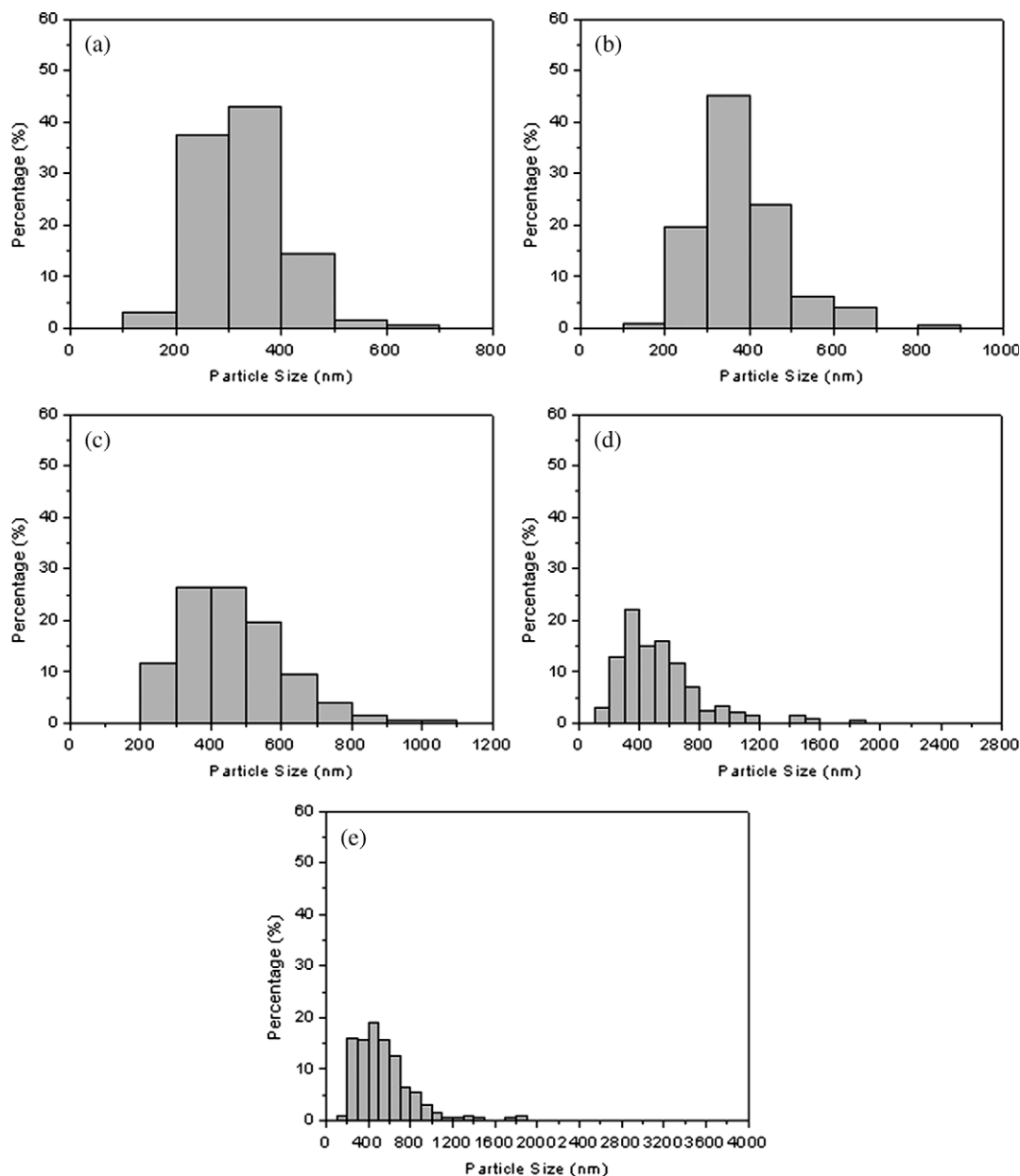


Figure 9 PSD of the precipitated PMMA particles for a PMMA MW of 85,000, a temperature of 298 K, a pressure of 6.41 MPa, a liquid CO₂ level in the precipitator of one-eighth, and PMMA concentrations of (a) 0.4, (b) 0.72, (c) 1, (d) 2, and (e) 4 wt %.

spraying, liquid CO₂ with a density of 0.80 g/cm³, and supercritical CO₂ with densities of 0.66 and 0.73 g/cm³. All densities were extracted from the NIST Chemistry Web Book.³² Figure 5 shows that nearly spherical, submicrometer-sized PMMA particles without coalescence were obtained by liquid CO₂ drying. When supercritical CO₂ was used as the drying agent after the spraying, the liquid CO₂ level dropped gradually, and the suspended particles fell from the liquid and were deposited onto the filter located at the bottom of the precipitator. Because of the intimate contact and depletion of mass from the retained solution among the precipitated particles, coalescence thus occurred. The observation therefore

suggests that a suspension of the particles in liquid for a certain period is required for drying.

Effect of the PMMA concentration

For the precipitation of PMMA with an MW of 36,000 from a toluene solution at 298 K and 6.41 MPa with a liquid CO₂ level of one-eighth, Figure 6 shows that mainly submicrometer-sized PMMA particles without coalescence were generated at a PMMA concentration equal to or less than 1 wt %. Figure 6 also shows that the average particle size increased with the PMMA concentration increasing in toluene. Besides, a wider PSD occurred for

toluene solutions containing higher PMMA concentrations, as shown in Figure 7. Because the injection rate of the PMMA solution was kept constant, a possible reason for the wider PSD is more difficult jet breakup due to the relatively low Weber numbers,³³ which resulted from an increase in the viscosity at high PMMA concentrations. As a result, large particles were generated. The same trend was also observed for the precipitation of COC from toluene with compressed HFC-134a as the antisolvent.³³ For the precipitation of PMMA with an MW of 85,000 under the same operation conditions used for PMMA with an MW of 36,000, the morphology and size as well as PSD of the collected PMMA particles are shown in Figures 8 and 9, respectively. Figure 8 also shows that submicrometer-sized PMMA particles without coalescence could be formed at a PMMA concentration equal to or less than 1 wt %, just as in the operation for PMMA with an MW of 36,000. In a comparison of the PSDs with these two MWs, we find from Figures 7 and 9 that a narrower PSD always occurred for the PMMA with an MW of 85,000, especially at higher PMMA concentrations. This occurred because the faster nucleation rate for the higher MW PMMA and the lower mass allowed participation in growth after the depletion of mass by nucleation at low PMMA concentrations. In all the runs, a yield greater than 90% was found, and the MW of the precipitated PMMA was observed to be sufficiently close to that of the parent PMMA, with the difference always less than 8%; this indicated the applicability of the operation.

CONCLUSIONS

Solid, submicrometer-sized PMMA particles without coalescence were generated in a continuous PCA operation in which a nozzle with an inner diameter of 0.25 mm was used for injection and both vapor and liquid CO₂ existed in a precipitator with an inner diameter of 0.05 m and a total volume of 600 mL. No stabilizer was present in the PMMA solution. At a temperature of 298 K, a pressure of 6.41 MPa, a solution flow rate of 5 mL/min, and a CO₂ flow rate of 2000 mL/min, a liquid CO₂ level in the precipitator of one-eighth was found to be the most appropriate level. Among the solvents used, toluene was found to be more appropriate than THF, acetone, and nitromethane because it possesses the smallest δ value. A solvent with a δ value less than that of the polymer and a large difference in the δ values between the solvent and polymer are therefore suggested in this study for the selection of the solvent for a PCA operation. After the spraying of the PMMA solution is finished, liquid CO₂ instead of supercritical CO₂ is suggested to dry the precipitated PMMA particles. To generate submicrometer-

sized PMMA particles with a more uniform PSD, the PMMA concentration in toluene should not be higher than 1.0 wt %. When the PMMA with the larger MW was used, a narrower PSD could be achieved because of the differences in the nucleation and growth rate during the precipitation.

References

1. Jung, J.; Perrut, M. *J Supercrit Fluids* 2001, 20, 179.
2. Shariati, A.; Peters, C. J. *Curr Opin Solid State Mater Sci* 2003, 7, 371.
3. Yeo, S. D.; Kiran, E. *J Supercrit Fluids* 2005, 34, 287.
4. Reverchon, E.; De Marco, I.; Torino, E. *J Supercrit Fluids* 2007, 43, 126.
5. Kim, J. H.; Paxton, T. E.; Tomasko, D. L. *Biotechnol Prog* 1996, 12, 650.
6. Benedetti, L.; Bertucco, A.; Pallado, P. *Biotechnol Bioeng* 1997, 53, 232.
7. Han, S. J.; Lohse, D. J.; Radosz, M.; Sperling, L. H. *J Appl Polym Sci* 2000, 77, 1478.
8. Sun, Y. P.; Guduru, R.; Lin, F.; Whiteside, T. *Ind Eng Chem Res* 2000, 39, 4663.
9. Blasig, A.; Shi, C.; Enick, R. M.; Thies, M. C. *Ind Eng Chem Res* 2002, 41, 4976.
10. Bertucco, A.; Lora, M.; Kikic, I. *AIChE J* 1998, 44, 2149.
11. Muhrer, G.; Mazzotti, M. *Biotechnol Prog* 2003, 19, 549.
12. Weber, A.; Yelash, L. V.; Kraska, T. *J Supercrit Fluids* 2005, 33, 107.
13. Dixon, D. J.; Johnston, K. P. *J Appl Polym Sci* 1993, 50, 1929.
14. Reverchon, E.; Della Porta, G.; Sannino, D.; Ciambelli, P. *Powder Technol* 1999, 102, 127.
15. Owens, J. L.; Anseth, K. S.; Randolph, T. W. *Macromolecules* 2002, 35, 4289.
16. Boutin, O.; Badens, E.; Carretier, E.; Charbit, G. *J Supercrit Fluids* 2004, 31, 89.
17. Gokhale, A.; Khusid, B.; Dave, R. N.; Pfeffer, R. *J Supercrit Fluids* 2007, 43, 341.
18. Reverchon, E.; De Marco, I.; Adami, R.; Caputo, G. *J Supercrit Fluids* 2008, 44, 98.
19. Vega, A.; Subra, P.; López, A. M.; García, C. A.; Domingo, C. *Eur Polym J* 2008, 44, 1081.
20. Zhang, J.; Liu, Z.; Han, B.; Li, Z.; Sun, D.; Chen, J. *Eur Polym J* 2004, 40, 1349.
21. Mawson, S.; Yates, M. Z.; O'Neill, M. L.; Johnston, K. P. *Langmuir* 1997, 13, 1519.
22. Young, T. J.; Johnston, K. P.; Mishima, K.; Tanaka, H. *J Pharm Sci* 1999, 88, 640.
23. Fan, H. A.; Tan, C. S. *Sep Sci Technol* 2004, 39, 3453.
24. Tan, C. S.; Lin, H. Y. *Ind Eng Chem Res* 1999, 38, 3898.
25. Reverchon, E.; Schiavo Rappo, E.; Cardea, S. *Polym Eng Sci* 2006, 46, 188.
26. Suzuki, H.; Hattori, Y.; Iizuka, T.; Yuzawa, K.; Matsumoto, N. *Thin Solid Films* 2003, 438-439, 288.
27. Liu, J.; Liu, T.; Kumar, S. *Polymer* 2005, 46, 3419.
28. Brandrup, J.; Immergut, E. H.; Grulke, E. A.; Abe, A.; Bloch, D. R. *Polymer Handbook*, 4th ed.; Wiley: Hoboken, NJ, 1999.
29. Marcus, Y. *J Supercrit Fluids* 2006, 38, 7.
30. Jessop, P. G.; Subramaniam, B. *Chem Rev* 2007, 107, 2666.
31. Zhou, X. D.; Zhang, S. C.; Huebner, W.; Ownby, P. D. *J Mater Sci* 2001, 36, 3759.
32. NIST Chemistry Web Book. Thermophysical properties of carbon dioxide. <http://webbook.nist.gov> (accessed December 2009).
33. Hsu, R. Y.; Tan, C. S.; Chen, J. M. *J Appl Polym Sci* 2002, 84, 1657.